

# Development of DNDC-BC model to estimate greenhouse gas emissions from rice paddy fields under combination of biochar and controlled irrigation management

Zewei Jiang<sup>a</sup>, Shihong Yang<sup>a,b,c,\*</sup>, Pete Smith<sup>d</sup>, Mohamed Abdalla<sup>d</sup>, Qingqing Pang<sup>e</sup>, Yi Xu<sup>a</sup>, Suting Qi<sup>a</sup>, Jiazhen Hu<sup>a</sup>

<sup>a</sup> College of Agricultural Science and Engineering, Hohai University, Nanjing, PR China

<sup>b</sup> State Key Laboratory of Hydrology-Water Resources and Hydraulic Engineering, Hohai University, Nanjing, PR China

<sup>c</sup> Cooperative Innovation Center for Water Safety & Hydro Science, Hohai University, Nanjing, PR China

<sup>d</sup> Institute of Biological & Environmental Sciences, University of Aberdeen, 23 St Machar Dr., Aberdeen AB24 3UU, UK

<sup>e</sup> Nanjing Institute of Environmental Sciences, Ministry of Ecology and Environment, Nanjing 210042, PR China

## ARTICLE INFO

Handling Editor: Diego Abalos

### Keywords:

Biochar  
Controlled irrigation paddy  
Model development  
Rice  
DNDC-BC  
Greenhouse gas emissions

## ABSTRACT

Simulating the impacts of biochar and controlled irrigation (CI, a water-saving irrigation technology without surface ponding of water) combination on greenhouse gas (GHG) emissions from paddy fields is crucial, however, the original DNDC model is not capable of capturing these management impacts on emissions. In this study, we have created a new modelling approach called DNDC-Biochar-Controlled Irrigation (DNDC-BC) by adding two modules to the original DNDC: the water balance principle, and the two-pool biochar model. The performance of the DNDC-BC was tested and validated using a two-year field experiment, designed with two irrigation treatments (flood irrigation (FI), and CI) and three biochar application rates (0, 20, and 40 t ha<sup>-1</sup>), carried in the Lake Taihu region, China. Results revealed that the DNDC-BC model performed satisfactorily in simulating impacts of biochar-CI combination on emissions of CH<sub>4</sub>, N<sub>2</sub>O, SOC, and grain yield. The corresponding R<sup>2</sup> values of DNDC-BC increased by 22.63%-35.66%, 43.00%-71.26%, 1.06%-60.87% and 15.38%-34.78% compared with those of the original model. Sensitivity analysis for the DNDC-BC showed that CH<sub>4</sub> emissions were most sensitive to rainfall and irrigation; N<sub>2</sub>O emissions were sensitive to rainfall, irrigation and N fertilizer application rate, and SOC was sensitive to biochar application rates. Our results suggest that the combination of biochar- and CI can save water resources and mitigate GHG emissions without detrimental impacts on rice yield. The DNDC-BC can be used to estimate the long-term impacts of biochar-CI combination on GHG emission, crop productivity and climate change.

## 1. Introduction

In the context of global warming, agricultural production needs to reduce its environmental footprint of greenhouse gas (GHG) emissions, including methane (CH<sub>4</sub>), carbon dioxide (CO<sub>2</sub>), and nitrous oxide (N<sub>2</sub>O), while meeting the demands of a growing population (Bradford et al., 2016; Carlson et al., 2016). Quantifying GHG emissions, soil organic carbon (SOC) and rice yield are essential for developing climate change mitigation methods and policies (Abdalla et al., 2020). However characterizing the complex interactions between crops, soils, management and environments across large temporal and spatial scales using only measurement studies can be extremely challenging and time

consuming (He et al., 2018). Fortunately, biogeochemical models have emerged as a reliable and cost-effective approach to help overcome these issues. Traditional statistical models are not suitable for simulating the soil C and N cycle under complex physiological and climatic conditions, but process-based models can solve this problem.

There is increasing urgency to find sustainable agricultural production methods for carbon sequestration and mitigation of GHG emissions. Rice is the staple food for more than half of the world's population (Islam et al., 2018), but is also an important source of GHG emissions, accounting for 19% and 11% of global agricultural CH<sub>4</sub> and N<sub>2</sub>O emissions, respectively (US-EPA, 2006). China has the second-largest rice planting area and produces the most rice in the world (Liang et al.,

\* Corresponding author at: College of Agricultural Science and Engineering, Hohai University, 8th Focheng West Road, Jiangning District, Nanjing, PR China.  
E-mail address: [ysh7731@hhu.edu.cn](mailto:ysh7731@hhu.edu.cn) (S. Yang).

2016), but the traditional flooding irrigation (FI) is still adopted by most paddy fields, which consumes more than 65% of the total agricultural irrigation water (Si et al., 2000). Thus, it is necessary to implement field management measures to save water and to reduce emissions from rice fields in China (Yang et al., 2019). Many water-saving measures, including controlled irrigation (CI) have been developed (Liang et al., 2017). CI, which determines the irrigation schedule based on the rhizosphere soil moisture, has been widely applied in China due to the potential benefits of reducing lodging susceptibility, better root development while saving water, and possibly reducing nutrient losses by lower water outflow (Peng et al., 2009; Song et al., 2019). However, this method may increase N<sub>2</sub>O emissions while saving water and reducing CH<sub>4</sub> emissions (Hou et al., 2012). In addition, various studies found that biochar is conducive to GHG mitigation, carbon storage, and pollution removal (Guo et al., 2020; Qi et al., 2020). As a low-cost negative emission technology, biochar can easily be obtained from agricultural wastes such as crop straw (He et al., 2019), and is widely used in carbon sequestration, yield boosting and soil fertility improvement (Lehmann, 2007). Therefore, the coupling of biochar and CI might be an important measure to address climate change and deal with the trade-off between CH<sub>4</sub> and N<sub>2</sub>O, but it is still difficult to simulate gas emissions under this combined management.

In contrast to these simpler models, the Denitrification Decomposition (DNDC) model represents a process-based framework that is able to simulate hydrological and biogeochemical cycles and has been widely validated and used worldwide (Abdalla et al., 2011; Li et al., 2014; Dubache et al., 2019). At present, most studies using the DNDC model to simulate GHG emissions from farmland have focused on the impact of traditional irrigation and tillage systems. However, although many studies have shown that the DNDC model has a good adaptability in China, only a few studies have focused on simulating the effects of biochar and even less have investigated the combined effects with controlled irrigation on GHG emissions and SOC of paddy fields were found in the literature. For example, using DNDC, Li et al. (1994) simulated significantly higher N<sub>2</sub>O emissions from organic soils compared to other farmlands. Reducing the drainage of organic fields, adopting precision irrigation and deep fertilization can significantly reduce N<sub>2</sub>O emissions.

The existing DNDC model cannot simulate GHG emissions under biochar and CI treatments. Modelling biochar is difficult due to its stability over the centennial or even millennium scale (Leng and Huang, 2018). Currently, the common methods to evaluate the stability of biochar include biochar carbon (C) structure and composition analysis, oxidation-resistance determination, incubation and modelling evaluation. Among them, only the last method can assess the long-term stability of biochar carbon and has been widely used. To simplify the problem, it is usually assumed that the biochar in soil decays exponentially, and one-pool and multi-pool models have been developed (Leng et al., 2019), showing the potential for introducing biochar into biogeochemical models such as DNDC. Further, the flood module of paddy fields in DNDC simulates only two types of management, continuous flooding and alternative wetting and drying, for which the water layer is stable at 10 cm and fluctuates between -5 cm and 5 cm respectively (Zhang and Niu, 2016). This is totally different to CI, which regulates irrigation amount through soil moisture content and has been widely used over recent decades, especially in China. Hence, it is necessary to improve the DNDC model to meet the requirements of modelling GHG emission from CI paddy fields under biochar application.

In this study, DNDC-Biochar-CI (DNDC-BC), an improved version of DNDC95, was developed to simulate GHG emissions from CI paddy fields under biochar application by introducing biochar modelling and water balance equations. The objectives of this study are: (1) to incorporate the water balance equations and the two-pool biochar model for the simulation of CI paddy systems under biochar application; (2) to test the ability of the DNDC-BC to simulate CH<sub>4</sub> and N<sub>2</sub>O emissions, soil

temperature and moisture, SOC, and rice yield under CI and biochar application; (3) to investigate the sensitivity of the model to input parameters for simulating CH<sub>4</sub>, N<sub>2</sub>O emissions, and SOC changes under the combination of CI and biochar application.

## 2. Materials and methods

### 2.1. Study site and experiment design

The experiment site is located at the State Key Laboratory of Hydrology-Water Resources and Hydraulic Engineering of Hohai University, Kunshan, China (34°63'21"N, 121°05'22"E). The test area has a southern subtropical monsoon climate zone, with a mean annual temperature of 15.5°C, precipitation of 1097.1 mm, evaporation of 1365.9 mm, sunshine duration of 2085.9 h, and frost-free season of 234 days. The local precipitation, temperature during the experimental period were recorded by Open Path Eddy Covariance (Campbell Scientific Ltd., USA) with an automatic-meteorological measurement system (WS-STD1, DELTAT, UK) and shown in Fig. S1. Net radiation and humidity data were also collected to the eddy covariance by CNR4 four-component net radiation meter and HMP155A air temperature and humidity probe, and the missing data were obtained from the Meteorological Information Center of China Meteorological Administration (<http://data.cma.gov.cn/>). The soil is classified as Hydragric Anthrosol with soil organic matter, total nitrogen (N), total phosphorus (P), total potassium (K) and pH (at 0–20 cm depth) of 21.71 g kg<sup>-1</sup>, 1.79 g kg<sup>-1</sup>, 1.4 g kg<sup>-1</sup>, 20.86 g kg<sup>-1</sup>, and 7.4, respectively, while bulk density (BD) at 0–30 cm depth is 1.32 g cm<sup>-3</sup>. The content of ammonium nitrogen (NH<sub>4</sub><sup>+</sup>-N), nitrate nitrogen (NO<sub>3</sub><sup>-</sup>-N), available phosphorus (AP) and available potassium (AK) in the soil before rice planting were 5.87 mg kg<sup>-1</sup>, 1.12 mg kg<sup>-1</sup>, 19.72 mg kg<sup>-1</sup>, and 126.20 mg kg<sup>-1</sup>, respectively.

The experiment was conducted in a drainage lysimeter (2.5 m × 2 m) from June 2016 to November 2017. There were four treatments with three replicates: rice-straw biochar at three addition levels (A, 0 t ha<sup>-1</sup>, B, 20 t ha<sup>-1</sup>, C, 40 t ha<sup>-1</sup>) with CI and 40 t ha<sup>-1</sup> biochar application with FI, named CA, CB, CC, and FC, respectively. The main properties of the biochar used in the experiment (Zhejiang Biochar Engineering Technology Research Center) are shown in Table S1. Biochar was evenly spread on the plots manually using shovel and hoe and incorporated into the soil at 0–20 cm before rice transplantation in 2016. No additional biochar was added in the following year. The conventional FI treatments were managed by local rice planting habits, maintaining 5–25 mm of water layer for the whole rice growing season except for the late tillering stage. The CI treatment, however, only retains 5–25 mm of water layer in the re-greening stage, and 60%–80% of saturated soil moisture content as the irrigation control index in other stages. No standing water layer was established except for pesticide and N fertilization under CI (Table 1). More details can be found in (Yang et al., 2019). The rice plant and row spacings were 13 cm and 25 cm, respectively, and the seedlings were 3–4 plants per hole. Rice was transplanted on June 30 and harvested on November 3 for the first rice season (2016), and the rice variety was *Nanjing 46*. In 2017, the rice was transplanted on June 30 and harvested on October 31. Application of N fertilizer was managed according to the local farmers' customary fertilization methods and amounts (Table S2).

### 2.2. Gas sampling, SOC and yield measurements

CH<sub>4</sub> and N<sub>2</sub>O were collected *in situ* by static chambers. The chambers made of PVC, 5 mm thick, with a cross-sectional area of 0.25 m<sup>2</sup> (50 cm × 50 cm) and height of 60 cm, were placed in each plot. The gas samples were collected every 5 days from the second day after rice transplantation till September of each year, and the sampling intervals increased to a week from September to harvest. The samples were collected on the 2nd, 4th, 6th, 8th days after fertilization. Samples were collected at 10 min intervals from 10:00 a.m. to 10:30 a.m. on each

**Table 1**  
Controlled thresholds in different stages for controlled irrigation.

Stages & DAP	Water management		
	CI	FI	Observed root zone depth (cm)
Regreening Stage (0–10 d)	5–25 mm	20–50 mm	—
Tillering Stage (11–20 d)	Initial 70–100% $\theta_{s1}$	20–50 mm	0–20
Middle (21–30 d)	65–100% $\theta_{s1}$	20–50 mm	0–20
Late (31–40 d)	60–100% $\theta_{s1}$	No standing water	0–20
Jointing and Booting Stage (41–55 d)	75–100% $\theta_{s2}$	20–50 mm	0–30
Heading and Flowering Stage (56–74 d)	80–100% $\theta_{s3}$	20–50 mm	0–40
Milk Stage (75–94 d)	70–100% $\theta_{s3}$	20–50 mm	0–40
Ripening Stage (95–116 d)	Naturally drying	Naturally drying	—

Note: DAP represents days after transplanting, CI and FI represent controlled irrigation and flood irrigation,  $\theta_{s1}$ ,  $\theta_{s2}$ , and  $\theta_{s3}$  represent average volumetric soil moisture for the 0–20, 0–30, and 0–40 cm soil layers, respectively.

sampling day. After sampling, gas samples were stored in a Tedlar airbag and analyzed within 3 days in the laboratory by a gas chromatography (Agilent 7890A, Agilent Technologies Ltd., USA). Soil moisture and temperature was recorded automatically (every half hour) by a soil water content automatic measurement system (HOBO S-SMxM005, Onset Computer Corp, USA) installed in each plot.

Rice yield was estimated by manually harvesting the plants per unit area of each plot. After threshing, the number of filled grain, setting percentage, thousand-kernel-weight, and panicle number of each treatment were calculated according to three randomly selected hills of rice. Soil samples (12 plots) of 0–10 cm, 10–20 cm, and 20–40 cm were collected in the regreening stage, tillering stage, jointing stage, and after harvest in 2016 and 2017. SOC content in different soil layers at different growth stages was measured by the potassium dichromate external heating method (De Feudis et al., 2019).

The  $\text{CH}_4$  and  $\text{N}_2\text{O}$  flux was calculated according to equation (1):

$$F = \rho \cdot h \cdot \frac{273}{273 + T} \frac{dC}{dt} \quad (1)$$

where  $F$  is the gas emission flux,  $\text{CH}_4$  is  $\text{mg m}^{-2}\text{h}^{-1}$ ,  $\text{N}_2\text{O}$  is  $\mu\text{g m}^{-2}\text{h}^{-1}$ ,  $\text{CO}_2$  is  $\text{mg m}^{-2}\text{h}^{-1}$ ;  $\rho$  is the density of  $\text{CH}_4$ ,  $\text{N}_2\text{O}$  and  $\text{CO}_2$  in the standard state, and their values are  $0.714 \text{ kg m}^{-3}$ ,  $1.977 \text{ kg m}^{-3}$ , and  $1.977 \text{ kg m}^{-3}$ , respectively;  $h$  is the height from the top of the chamber to the surface water layer, m;  $T$  is the average temperature in the chamber,  $^{\circ}\text{C}$ ;  $\frac{dC}{dt}$  is the change rate of gas concentration ( $\text{CH}_4$  is  $\text{mg m}^{-3}\text{h}^{-1}$ ,  $\text{N}_2\text{O}$  is  $\mu\text{g m}^{-3}\text{h}^{-1}$ ), which is determined by the fitting line slope of four gas samples densities in each group and the corresponding sampling time of 0, 10, 20 and 30 min.

The cumulative emissions of GHG were calculated by the following equation:

$$E_s = \sum (F_{i+1} + F_i) / 2 \times 24 \times (d_{i+1} - d_i) \quad (2)$$

where  $E_s$  is the seasonal emission flux of GHG;  $F_i$  is the gas emission flux of the  $i$ -th sampling;  $d_i$  is the sampling date,  $n$  is the number of GHG sampling.

## 2.3. DNDC model

### 2.3.1. Model description

The DNDC is a biogeochemical model for simulating C and N cycles in agricultural systems and can be used to estimate SOC, crop growth, ammonia ( $\text{NH}_3$ ) volatilization, dinitrogen ( $\text{N}_2$ ) and GHG ( $\text{CO}_2$ ,  $\text{CH}_4$ ,  $\text{N}_2\text{O}$ ) emissions from soils (Li et al., 1992a; Li et al., 1992b). Since its

establishment, DNDC has been used worldwide to simulate various crop and management practices and is being continuously improved and developed (Gilhespy et al., 2014). The biochemical sub-module of DNDC includes nitrification, fermentation and denitrification. The model was designated as the first biogeochemical model in the 2000 Asia Pacific Global Change International Symposium (Chen et al., 2009). The DNDC model has shown a good ability to track trace GHG, mainly through the anaerobic balloon method to simulate the generation, oxidation, and transport of  $\text{CH}_4$  and  $\text{N}_2\text{O}$  gases. In brief, the anaerobic decomposition rate and methane metabolism rate were calculated by the decomposition rate of SOC and secretion rate of plant roots. The production of  $\text{CH}_4$  and  $\text{N}_2\text{O}$  was dependent on the estimation of DOC,  $\text{NO}_3^-$  and  $\text{NH}_4^+$  substrates. More details are available in previous literature (Zhang and Niu, 2016; Shaukat et al., 2022). In this study, DNDC v9.5 (<https://www.dndc.sr.unh.edu/>) was used and the source code was modified to realize the simulation of GHG emissions from CI paddy fields under biochar application. There are only three default settings for paddy field irrigation, namely, rainfed, traditional flooding, and alternation wetting and drying (water level fluctuates between  $-5 \text{ cm}$  and  $5 \text{ cm}$ ), which are different from the CI management controlled by moisture content. While in the manure amendment module, the commonly straw, organic fertilizer and other inputs are available, and the SOC will decompose quickly. It is not appropriate to simulate the biochar with the sequestration scale for more than 100 years.

### 2.3.2. Model input parameters

Model inputs consists meteorological data, soil data and management data. The historical meteorological data from 1961 to 2020 were obtained from the Meteorological Information Center of China Meteorological Administration (<http://data.cma.cn/>), including daily maximum temperature, minimum temperature, radiation, wind speed, and precipitation. The experimental data of 2016 and 2017 were used to calibrate and validate the model respectively. The details on model calibration can be found in Section 2.6. Basic soil parameters such as initial SOC content, soil type, pH and BD were based on the measured values. The timing and amounts for N Fertilization application, irrigation and biochar amendments along with the tillage type and timings were all input in accordance to observed data. Other parameters were optimized based on the trial-and-error method where the RMSE for simulated  $\text{CH}_4$ ,  $\text{N}_2\text{O}$  emissions, SOC in 2016 was minimized, as shown in Table 2.

## 2.4. Model improvements

### 2.4.1. Development of DNDC-BC

On the basis of the DNDC95 model and our previous study (Jiang et al., 2021a), this study further improved the flood irrigation module and the manure module to develop DNDC-BC, by mainly including two extra processes: (1) added the CI module based on the principle of water balance, (2) added the biochar fertilizer module based on biochar modelling. The structure of the DNDC-BC model is shown in Fig. 1. Specifically, to meet the needs of aquifer irrigation under CI management, the balance relationship of rainfall, irrigation, evapotranspiration, runoff, infiltration and water level fluctuation was used to calculate the irrigation amount when the lower limit was reached, and no irrigation was applied except during N fertilizer, pesticide and insecticide application periods. It is noticeable when fertilizer or pesticide are applied, irrigation was supplemented to maintain the 5 cm water table. In addition, the original mode of water level dynamics was changed to operate on the basis of upper and lower limits of soil moisture content. Different fluctuation range of water level was set up within the depth of rice root according to the requirements of CI technology for different growth stages of rice (Table 1). The irrigation of CI treatment based on water balance was calculated as follows.

$$WT_n - WT_{n-1} = Irri_n + P_n - ET_n - Inf_n - R_n \quad (3)$$

**Table 2**  
Main input parameters of crop and biochar used in DNDC model.

Groups	Parameters	Values
Soil	Land-use type	Rice paddy field
	Soil texture	Clay
	Bulk density (g cm <sup>-3</sup> )	1.36
	Soil pH	7.4
	Field capacity (cm <sup>-1</sup> )	0.75
	Clay fraction (cm <sup>-1</sup> )	0.11
	Initial SOC (kg kg <sup>-1</sup> )	0.01
	Accumulated temperature (°C) <sup>a</sup>	3000
Crops	Maximum biomass production of grain (kg C ha <sup>-1</sup> y <sup>-1</sup> )	4200
	Optimum temperature (°C)	25.0
	N fixation index	1.05
	Depth of root active layer in the initial stage (m)	0.2
	Depth of root active layer in the middle stage (m)	0.3
	Depth of root active layer in the end-stage (m)	0.4
Irrigation	Leak water of CI (mm d <sup>-1</sup> )	3.0
	Leak water of FI (mm d <sup>-1</sup> )	5.0
Biochar	Applied depth (cm)	20
	Biochar pH	10.2
	Absorption ratio (AR)	0.2
	Labile biochar rate (LBR)	0.1
	Mean residence time (MRT) of labile biochar pool (MRT <sub>L</sub> )	500
	MRT of labile biochar pool (MRT <sub>R</sub> )	1000
	Organic carbon of biochar (kg C t <sup>-1</sup> ha <sup>-1</sup> )	4260
	Organic nitrogen of biochar (kg N t <sup>-1</sup> ha <sup>-1</sup> )	65.54

Note: <sup>a</sup> Accumulated temperature was calculated based on optimum temperature (°C).

$$Irri_n = \begin{cases} 0, & Mois \geq Mois_{min} \\ WT' - WT_n, & Mois < Mois_{min} \end{cases} \quad (4)$$

$$R_n = \begin{cases} 0, & WT \leq WT_{max} \\ WT - WT_{max}, & WT > WT_{max} \end{cases} \quad (5)$$

where  $WT_n$  and  $WT_{n-1}$  represent the water level of  $n$  days and  $n-1$  days (mm), respectively,  $Irri_n$ ,  $P_n$ ,  $ET_n$ ,  $Inf_n$ , and  $R_n$  represent irrigation, precipitation, ET, infiltration, and runoff at day  $n$ , respectively (units: mm day<sup>-1</sup>).  $Mois$  and  $Mois_{min}$  represent the current soil moisture and the lower limit of irrigation in each growth period under CI treatment.  $WT'$

represent the upper limit of irrigation set by CI and is 3–5 cm in most growth periods (Table 1).  $WT_{max}$  represent the ponding water level and the height of the ridge of the paddy field or the lowest value of artificial drainage. ET was calculated by the daily version (Allen & Pereira, 1998) rather than the hourly version (Allen et al., 2006) of FAO-56 Penman-Monteith equation for daily timesteps which was inserted in the DNDC95 model.

Biochar was introduced into the modified DNDC model as a new type of manure. Considering its alkalinity, porous structure and carbon stability, its pH, adsorption rate and carbon pools were established, respectively. The C/N ratio, organic carbon content, organic nitrogen content, pH, NH<sub>4</sub><sup>+</sup>-N content and NO<sub>3</sub><sup>-</sup>-N content of biochar were input in the modified model (DNDC-BC). In addition, we have added four key parameters, including absorption ratio (AR), labile biochar rate (LBR), mean residence time (MRT) of labile biochar pool (MRT<sub>L</sub>), MRT of recalcitrant biochar pool (MRT<sub>R</sub>). Those parameters were optimized based on fitting to observation data and trial-and-error method (Table 2). More details are given in part 2.4.2 below. The DNDC-BC, an example file and basic introduction can be found at website of GitHub (<https://github.com/jzw787/DNDC-Biochar-CI/tree/main/DNDC>).

We compared the performance of the DNDC-BC-model to the DNDC95 model. However, since the DNDC95 model does not have a function for simulating GHG emissions under biochar and CI irrigation, sewage sludge in the manure amendment module was used to realize biochar input. The C/N ratio, carbon, and nitrogen content of organic fertilizer were modified to the actual values of biochar. The alternative wet and dry flooding was used to represent CI (Table 2). Other parameters were also optimized by the trial and error method.

#### 2.4.2. Biochar modelling

Considering the long-term effectiveness of biochar with a half-life of hundreds or even thousands of years, and the longest biochar incubation test at present is only 10 years (Kuzyakov et al., 2014), the long-term fate of biochar can only be estimated through modelling. There are three widely used biochar modelling methods, namely one-pool, two-pool and three-pool. According to a previous study (Leng et al., 2019), the one-pool model, also known as the one-exponential model, is too simple, while the three pools model has not been well validated. Therefore, the two-pool model was used in this study. In short, the two-pool model simplifies the chemical structure and arrangements of biochar into a relatively labile C pool and a refractory C pool. The

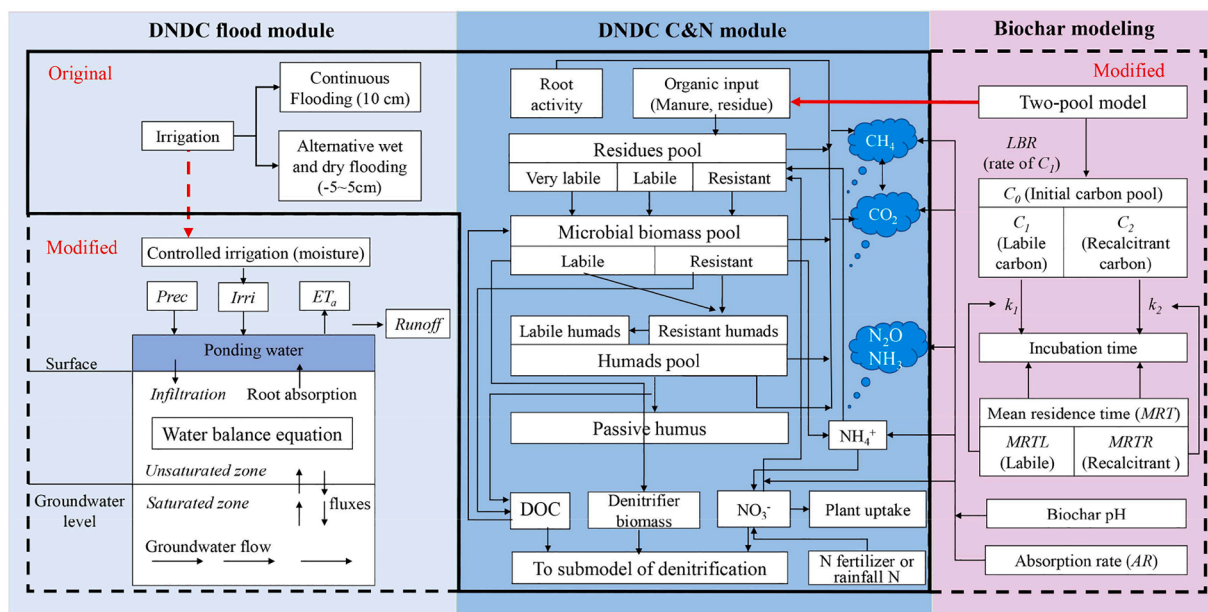


**Fig. 1.** The concepts module of the modified DNDC model, DNDC-BC, in which the original model was from the existing research (Li et al., 1992a).

mineralization characteristics of these two pools are different. The recalcitrant C pool is the major body of biochar, which is resistant to mineralization and has a residence time of several centuries, while the labile C pool is small and easy to mineralize, and its residence time is within a few years to decades (Leng et al., 2019). More details of the one-pool and the three-pool model can be found in the [supplementary materials](#). The two-pool model can be expressed as follows (Singh et al., 2012).

$$C_r = C_1 * \exp(-k_1 * t) + C_2 * \exp(-k_2 * t) \quad (6)$$

$$C_m = C_1 * [1 - \exp(-k_1 * t)] + C_2 * [1 - \exp(-k_2 * t)] \quad (7)$$

$$C_1 + C_2 = C_0 \quad (8)$$

where  $C_r$ ,  $C_m$ , and  $C_0$  represent biochar C remaining, mineralized at time  $t$ , and the initial amount in the soil, respectively.  $C_1$  and  $C_2$  represent labile and recalcitrant biochar C pool size, respectively. While  $k_1$  and  $k_2$  represent the mineralization rates of labile and recalcitrant biochar C pool, respectively, which could be calculated as following:

$$k_1 = 1/MRT_1 \quad (9)$$

$$k_2 = 1/MRT_2 \quad (10)$$

$$\begin{cases} MRT > 1000, H/C_{org} < 0.4 \\ 500 < MRT < 1000, 0.4 < H/C_{org} < 0.7 \end{cases} \quad (11)$$

where  $MRT_1$  and  $MRT_2$  denotes mean resident time of the labile and recalcitrant C pools (years), respectively.  $H/C_{org}$  represents the ratio of hydrogen and organic C content of biochar. The formula of  $MRT$  was according to a global dataset collected in a previous study (Lehmann and Joseph, 2009).

To integrate biochar modelling with DNDC model, as mentioned above, biochar was added as a new type of manure in the module of “Manure amendment”, which can input soil C/N ratio, manure pH, organic C, organic N,  $NH_4^+$ -N,  $NO_3^-$ -N, AR, LBR,  $MRT_L$ , and  $MRT_R$ , etc. AR represents the porous structure of biochar, which can absorb GHGs, and nitrogen. In brief, AR represents the proportion of input  $NH_4^+$ ,  $NO_3^-$ , and DOC decomposed by carbon input that is absorbed by biochar. As they are the precursors of  $N_2O$  and  $CH_4$ , this will affect GHG emissions and nitrogen dynamics. While LBR represents the proportion of  $C_1$  in  $C_0$ ,  $MRT_L$  and  $MRT_R$  correspond to  $MRT_1$  and  $MRT_2$ , respectively. In addition, the module of SOC was also modified, mainly because when biochar was applied, the value of DOC generated by fertilizer was changed to the value of dynamic change over time, that is, the difference between the carbon content of biochar and  $C_r$ . To simplify the input of biochar, the organic carbon content needs to be input manually, and other main parameters are automatically calculated in proportion and filled in the input text box.

## 2.5. Evaluation of DNDC-BC model

In this study, four widely used statistical criteria, including coefficient of model efficiency (EF), root mean square error (RMSE), relative root mean square error (nRMSE) and coefficient of determination ( $R^2$ ) were used to evaluate the DNDC-BC performance (Smith et al., 2020):

$$EF = 1 - \frac{\sum_{i=1}^n (SM_i - OBS_i)^2}{\sum_{i=1}^n (OBS_i - \overline{OBS})^2} \quad (12)$$

$$RMSE = \sqrt{\frac{\sum_{i=1}^n (OBS_i - SM_i)^2}{n}} \quad (13)$$

$$nRMSE = \frac{RMSE}{OBS_{avg}} \times 100 \quad (14)$$

$$R^2 = \left( \frac{\sum_{i=1}^n (OBS_i - OBS_{avg})(SM_i - SM_{avg})}{\sqrt{\sum_{i=1}^n (OBS_i - OBS_{avg})^2 \sum_{i=1}^n (SM_i - SM_{avg})^2}} \right)^2 \quad (15)$$

where  $OBS_i$  is the observed value;  $OBS_{avg}$  is the average observed value;  $SM_i$  is the simulated value;  $SM_{avg}$  is the average simulated value;  $n$  is the sample size. The closer  $R^2$  is to 1, the better the linear correlation between observed and simulated is. The smaller the value of nRMSE is, the higher the fitting degree between the simulated and observed values. According to a previous study (Yang et al., 2014), when the nRMSE is less than 15% and more than 30%, it represents “good” and “poor” agreement respectively, while 15%-30% means “moderate” agreement.

## 2.6. Sensitivity analysis of DNDC-BC

Monte Carlo simulation was built into the DNDC95 model to analyse uncertainty due to input data. In this study, precipitation ( $mm\ y^{-1}$ ), atmospheric  $CO_2$  (ppm), atmospheric temperature ( $^{\circ}C$ ), soil porosity, water-filled pore space, initial SOC content ( $kg\ C\ kg^{-1}$ ), biochar amounts ( $kg\ C\ ha^{-1}$ ), urea fertilization ( $kg\ N\ ha^{-1}$ ) and irrigation (mm) parameters were used to test the sensitivity for estimating  $CH_4$ ,  $N_2O$  emissions and SOC in paddy fields. However, for DNDC-BC, sensitivity index (SI) was used to evaluate the results according to equation (16) (Zhao et al., 2016). Specifically, each input parameter was run 500 times in the analysis by randomly changing the selected parameters within a range of  $\pm 20\%$  while keeping other parameters unchanged (Table S3). The sensitivity of the selected input parameters was evaluated by selecting those results, including  $CH_4$ ,  $N_2O$  emissions, and SOC.

$$SI = \frac{(R_{Pmax} - R_{Pmin})/R_{Pavg}}{(P_{max} - P_{min})/P_{avg}} \quad (16)$$

where  $P_{max}$ ,  $P_{min}$ , and  $P_{avg}$  are the maximum, minimum, and average values of input parameters;  $R_{Pmax}$ ,  $R_{Pmin}$ , and  $R_{Pavg}$  are the corresponding simulation results, respectively.

## 2.7. Application attempts of DNDC-BC in other sites

Due to the lack of experimental data on SOC and biochar pools in paddy fields after long-term biochar application, we collected a dataset consisting of 22 long-term sets from 2010 to 2019 by retrieval (Table S6), referring to the approach of a previous study (Yin et al., 2022). Then the ability to apply DNDC-BC to other sites was tested. Detailed information about the dataset and related validation procedure could be found in [supplementary materials](#).

## 3. Results

### 3.1. Soil temperature and moisture

Accurate simulation of soil environmental factors such as temperature and moisture are the prerequisite for modelling GHG emissions. As illustrated in Fig. 2, the DNDC-BC model (the blue curves) captures the dynamics of soil temperature and moisture at 5 cm and 10 cm depth in each treatment. By contrast, the simulated soil temperature by the original model (the black curves) showed a lot of fluctuation, and it was difficult to predict the change of water content under CI, which once again proved the difference between CI and alternative drying and wetting irrigation. The  $R^2$  of soil temperature and moisture results predicted by the DNDC-BC model ranged from 0.90 to 0.97 and 0.59–0.92, respectively. These were 1.64%–16.41% and 0.07–14.48 times higher than that of the DNDC95 model. Specifically, the performance of DNDC-BC in different soil layers was generally satisfactory, but it was better in the top layer. The modified model achieved significantly better simulation results, but the soil temperature of the 10 cm soil layer

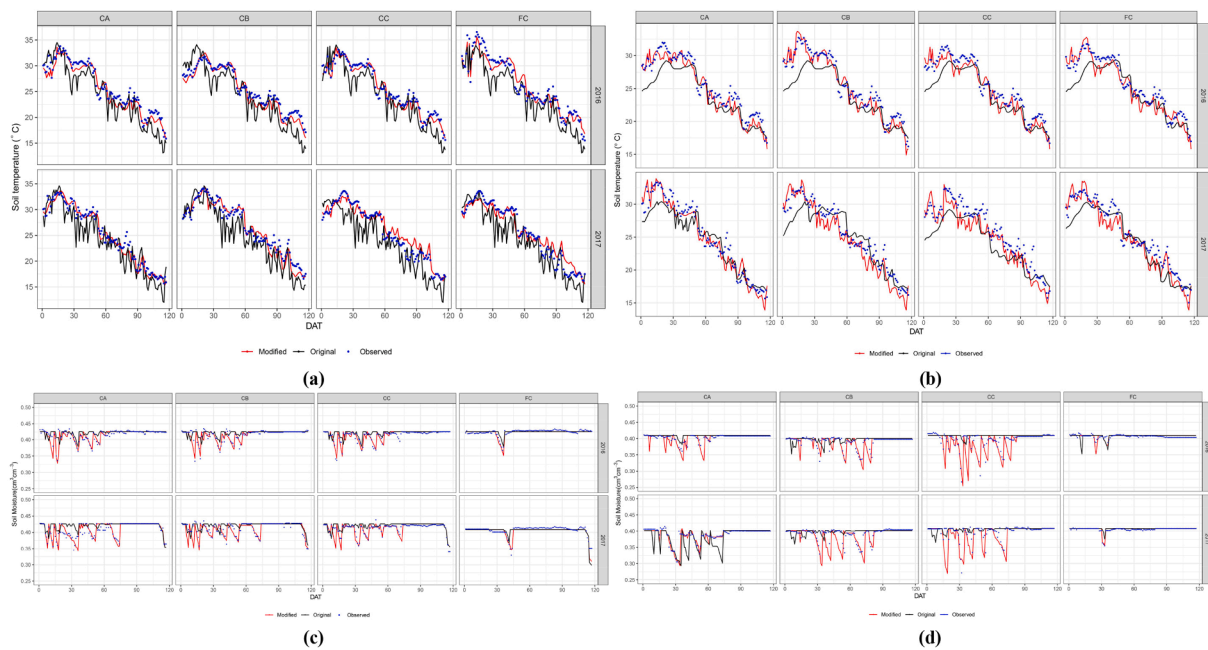


**Fig. 2.** Simulated soil temperature at 5 cm and 10 cm depths (a, b) and soil moisture at 5 cm and 10 cm depths (c, d) by the original model and modified DNDC model. 2016 and 2017 represent calibration and validation years respectively.

was still underestimated to some extent. The corresponding *nRMSE* for the DNDC95 were 4.06%–5.60% and 1.15%–6.40% higher (Tables 3 and 4). In addition, the *RMSE* values of DNDC-BC were lower by 18.62%–62.81% and 4.38%–56.36% respectively, compared to the original model. Overall, the DNDC-BC model worked better in simulating both soil moisture content and soil temperature compared to the original model.

### 3.2. CH<sub>4</sub> and N<sub>2</sub>O emissions

As shown in Fig. 3, DNDC-BC, effectively predicted CH<sub>4</sub> and N<sub>2</sub>O emissions from CI and FI paddy fields under different biochar applications rates. Application of biochar under CI treatment resulted in mitigating CH<sub>4</sub> and N<sub>2</sub>O emissions by 6.35%–29.9% and 11.64%–58.0% (except for CB in 2016 increased by 65.45%), respectively. The cumulative GHG emissions simulated by DNDC-BC were closer to the observed values than DNDC95. The observed (modified and original)

CH<sub>4</sub> and N<sub>2</sub>O emissions of CA, CB, CC and FC were 53.10–605 (38.98–587.10, 86.88–688.69) kg C ha<sup>-1</sup> and 1.67–8.67 (2.61–8.75, 2.16–9.00) kg N ha<sup>-1</sup> respectively. The simulations of CH<sub>4</sub> and N<sub>2</sub>O emissions for the calibration and validation periods are shown in Table 5. The *nRMSE* of CH<sub>4</sub> and N<sub>2</sub>O were 9.39%–22.65% and 4.31%–16.79%, and *R*<sup>2</sup> values were 0.79–0.93 and 0.84–0.97, respectively. The model efficiency factor was 0.8. The performance of the modified model was significantly improved in comparison with the original one. Here, *R*<sup>2</sup> values of CH<sub>4</sub> and N<sub>2</sub>O simulated by the DNDC-BC model increased by 22.63%–71.26% and the *RMSE* decreased by 7.19%–66.82%, respectively.

### 3.3. SOC and rice yield

Fig. 4 shows comparisons between observed and simulated SOC and rice yield under biochar by the DNDC95 and the DNDC-BC models. In general, the DNDC-BC model simulated SOC and rice yield under

**Table 3**  
Statistical criteria for simulation of soil temperature.

Soil layers	Years	Treatments	N	<i>R</i> <sup>2</sup>		RMSE		<i>nRMSE</i> (%)		EF	
				DNDC-BC	DNDC	DNDC-BC	DNDC	DNDC-BC	DNDC	DNDC-BC	DNDC
0–5 cm	2016	CA	117	0.96	0.88	1.17	2.54	4.62	10.39	0.94	0.70
		CB	117	0.97	0.84	1.04	2.78	4.12	11.47	0.93	0.61
		CC	117	0.96	0.89	1.02	2.40	4.06	9.93	0.95	0.72
		FC	117	0.94	0.92	1.28	2.68	4.86	11.01	0.94	0.74
	2017	CA	117	0.96	0.87	1.09	2.49	4.35	10.40	0.96	0.79
		CB	117	0.95	0.89	1.17	2.64	4.44	10.64	0.94	0.70
		CC	117	0.94	0.81	1.42	3.13	5.48	13.25	0.92	0.63
		FC	117	0.95	0.88	1.44	2.63	5.60	11.05	0.93	0.77
5–10 cm	2016	CA	117	0.94	0.91	1.28	2.00	5.13	8.44	0.99	0.97
		CB	117	0.96	0.88	1.17	2.31	4.62	9.77	0.93	0.72
		CC	117	0.93	0.92	1.31	1.84	5.32	7.78	0.89	0.78
		FC	117	0.91	0.86	1.37	1.81	5.44	7.65	0.88	0.77
	2017	CA	117	0.94	0.93	1.40	1.84	5.65	7.60	0.93	0.88
		CB	117	0.95	0.83	1.53	1.96	6.24	7.99	0.90	0.82
		CC	117	0.90	0.87	1.81	2.43	7.34	10.19	0.83	0.68
		FC	117	0.93	0.89	1.54	1.89	6.21	7.81	0.89	0.84

**Note:** N denotes the sample size. The RMSE units of soil temperature are °C<sup>-1</sup>. 2016 and 2017 represent calibration and validation years respectively. CA, CB, CC, and FC represent 0, 20, 40, 40 t ha<sup>-1</sup> biochar application with CI (C) and FI (F), respectively.

**Table 4**  
Statistical criteria for simulation of soil moisture.

Soil layers	Years	Treatments	N	R <sup>2</sup>		RMSE		nRMSE (%)		EF	
				DNDC-BC	DNDC	DNDC-BC	DNDC	DNDC-BC	DNDC	DNDC-BC	DNDC
0–5 cm	2016	CA	117	0.66	0.20	0.01	0.02	2.92	4.05	0.63	0.31
		CB	117	0.59	0.04	0.03	0.03	6.57	7.51	0.57	0.23
		CC	117	0.81	0.12	0.01	0.02	1.97	4.44	0.79	0.11
		FC	117	0.85	0.76	0.00	0.01	1.15	1.36	0.78	0.69
	2017	CA	117	0.79	0.16	0.01	0.02	2.85	5.74	0.72	0.22
		CB	117	0.63	0.28	0.01	0.02	3.34	4.32	0.50	0.12
		CC	117	0.68	0.42	0.01	0.02	2.90	3.75	0.53	0.17
		FC	117	0.83	0.42	0.01	0.01	1.99	3.51	0.75	0.22
5–10 cm	2016	CA	117	0.65	0.21	0.04	0.05	9.53	11.30	0.63	0.19
		CB	117	0.58	0.05	0.02	0.02	4.77	5.17	0.56	0.21
		CC	117	0.71	0.13	0.03	0.03	8.43	7.05	0.64	0.29
		FC	117	0.84	0.78	0.01	0.01	1.68	2.22	0.83	0.76
	2017	CA	117	0.66	0.37	0.01	0.03	3.73	7.31	0.66	0.55
		CB	117	0.61	0.35	0.02	0.03	5.41	7.01	0.51	0.12
		CC	117	0.69	0.37	0.02	0.03	5.79	8.79	0.56	0.21
		FC	117	0.92	0.65	0.01	0.01	0.69	1.49	0.87	0.40

**Note:** N denotes the sample size. The RMSE units of soil moisture are 1, respectively. 2016 and 2017 represent calibration and validation years respectively. CA, CB, CC, and FC represent 0, 20, 40, 40 t ha<sup>-1</sup> biochar application with CI (C) and FI (F), respectively.

different biochar application rates and water irrigation better than the DNDC95 model. Biochar amendment under CI increased SOC and rice yield by 4.25%–19.27% and 9.35%–15.85%, respectively. For SOC, the R<sup>2</sup>, RMSE and nRMSE of the original model and DNDC-BC were 0.54–0.94 and 0.72–0.96, 0.30–1.42 kg C kg<sup>-1</sup> and 0.10–0.48 kg C kg<sup>-1</sup>, 2.78%–13.22% and 0.87%–5.80%, respectively during the calibration period (Table S4). During the validation period, those values were 0.46–0.84 and 0.68–0.95, 0.39–1.85 kg C kg<sup>-1</sup> and 0.23–1.03 kg C kg<sup>-1</sup>, 4.72%–16.59% and 2.68%–9.09%, respectively. In general, the model has achieved satisfactory performance in SOC simulation of different soil layers, and captured the trend of SOC decreasing with the increase of soil depth. For rice yield, the R<sup>2</sup>, RMSE, and nRMSE of the DNDC-BC were 0.90–0.93, 359.86–994.40 kg ha<sup>-1</sup>, and 4.51%–13.57%, whilst the corresponding values of DNDC95 were 0.69–0.78, 483.01–585.01 kg ha<sup>-1</sup>, and 6.82%–8.33%, respectively (Table S5). Compared to the DNDC95, R<sup>2</sup> of simulated SOC and rice yield by the DNDC-BC increased by 1.06%–60.87% and 15.38%–34.78%, and RMSE decreased by 4.12%–33.47% and 17.44%–63.81%, respectively. Moreover, as illustrated in Fig. 6, the DNDC-BC could also be used for SOC simulation in other sites (including Ningxia, Jiangsu, and Guangdong), and the model achieved satisfactory results (R<sup>2</sup> = 0.88, RMSE = 1.54 g kg<sup>-1</sup>, nRMSE = 7.87%).

### 3.4. Sensitivity analysis

The sensitivity of DNDC-BC to input parameters was also investigated. Overall, irrigation and precipitation are the most important factors affecting CH<sub>4</sub>, N<sub>2</sub>O emissions, and SOC however, SOC is also sensitive to biochar application rate. A radar chart of sensitivity index (Fig. 5), showed that CH<sub>4</sub> emission from paddy fields was sensitive to increasing soil porosity, precipitation, atmospheric CO<sub>2</sub> and air temperature. By contrast, N<sub>2</sub>O emission was sensitive to irrigation, precipitation, field capacity, and urea fertilization. Among which, N<sub>2</sub>O emission from paddy fields was negatively correlated with atmospheric CO<sub>2</sub> concentration and soil porosity, and positively correlated with other factors. SOC was negatively correlated with precipitation, initial SOC content, and atmospheric temperature, but positively correlated with irrigation, atmospheric CO<sub>2</sub>, soil porosity, field capacity, urea fertilization and biochar application rate.

## 4. Discussion

### 4.1. Effects of biochar and CI on GHG emissions

Biochar and CI, as one technical means of the negative carbon

emission and water-saving irrigation (WSI), respectively, both have been vigorously promoted in Asia, especially in China in the past decades. With the goal of achieving carbon neutrality, alleviating water scarcity and ensuring food security become significant and urgent, more and more scholars (Akhtar et al., 2014; Yang et al., 2019; Haque et al., 2021) have investigated the effects of coupling biochar and CI techniques on GHG emissions, SOC and yield. It has been shown that CI reduces cumulative CH<sub>4</sub> emissions from paddies by 81.8% but increases cumulative N<sub>2</sub>O emissions by 135.4% (Hou et al., 2012), and biochar adsorption mitigates N<sub>2</sub>O emissions by 56.8%–90.1%. This study showed that the combined application of those two management systems can simultaneously achieve reductions in CH<sub>4</sub> and N<sub>2</sub>O emission by up to 29.9% and 58.0%, respectively. This was mainly because biochar prolonged the duration of denitrification, increased the abundance of narG gene and decreased the abundance of nosZ gene. However, the abundance of nosZ increases in the later stage, thus promoting the transformation from N<sub>2</sub>O to N<sub>2</sub> and reducing N<sub>2</sub>O emissions (Li et al., 2021). The mitigating effect of biochar on CH<sub>4</sub> emission is related to the change of pH, oxygen-containing functional groups and the activity of CH<sub>4</sub> oxidizing bacteria (Nan et al., 2021).

To further explore the effects of biochar on denitrification magnitude, methanogens, substrate availability and soil environment, the soil-trace gas processes simulated by DNDC-BC in 2016 (Fig. S2) and 2017 (Fig. S3) were analysed. It was found that the application of biochar changed the substrate availability and slightly increased soil pH. Specifically, the concentration of NO<sub>3</sub><sup>-</sup>-N, an important electron acceptor in the denitrification process, decreased by 4.72%–46.03%, and the concentration of NH<sub>4</sub><sup>+</sup>-N and DOC increased by 14.15%–33.98% and 34.56%–201.76%, respectively. A previous study (Fidel et al., 2017) has found that the decreased NO<sub>3</sub><sup>-</sup>-N and increased soil NH<sub>4</sub><sup>+</sup>-N and DOC concentrations may lead to the inhibition of N<sub>2</sub>O emission (Fig. 3), which is consistent with this study. Except for CB in 2016, biochar decreased denitrification and methanogens by 28.39%–69.03% and 4.38%–12.69% respectively, while FI increased methanogenic activity by 26.49%–42.34%. This partly revealed the reasons for the mitigation of CH<sub>4</sub> emissions by biochar and FI. It is worth noting that denitrification of CB (0.99 kg N ha<sup>-1</sup>) showed a peak higher than CA (0.45 kg N ha<sup>-1</sup>) 23 days after transplanting in 2016, which may be because CB treatment had no irrigation for more than 4 days during this period, and the impact of irrigation exceeded that of biochar. This was discussed in our previous study (Yang et al., 2019). Overall, DNDC-BC captured the dynamics of soil microbial activities and environment well.

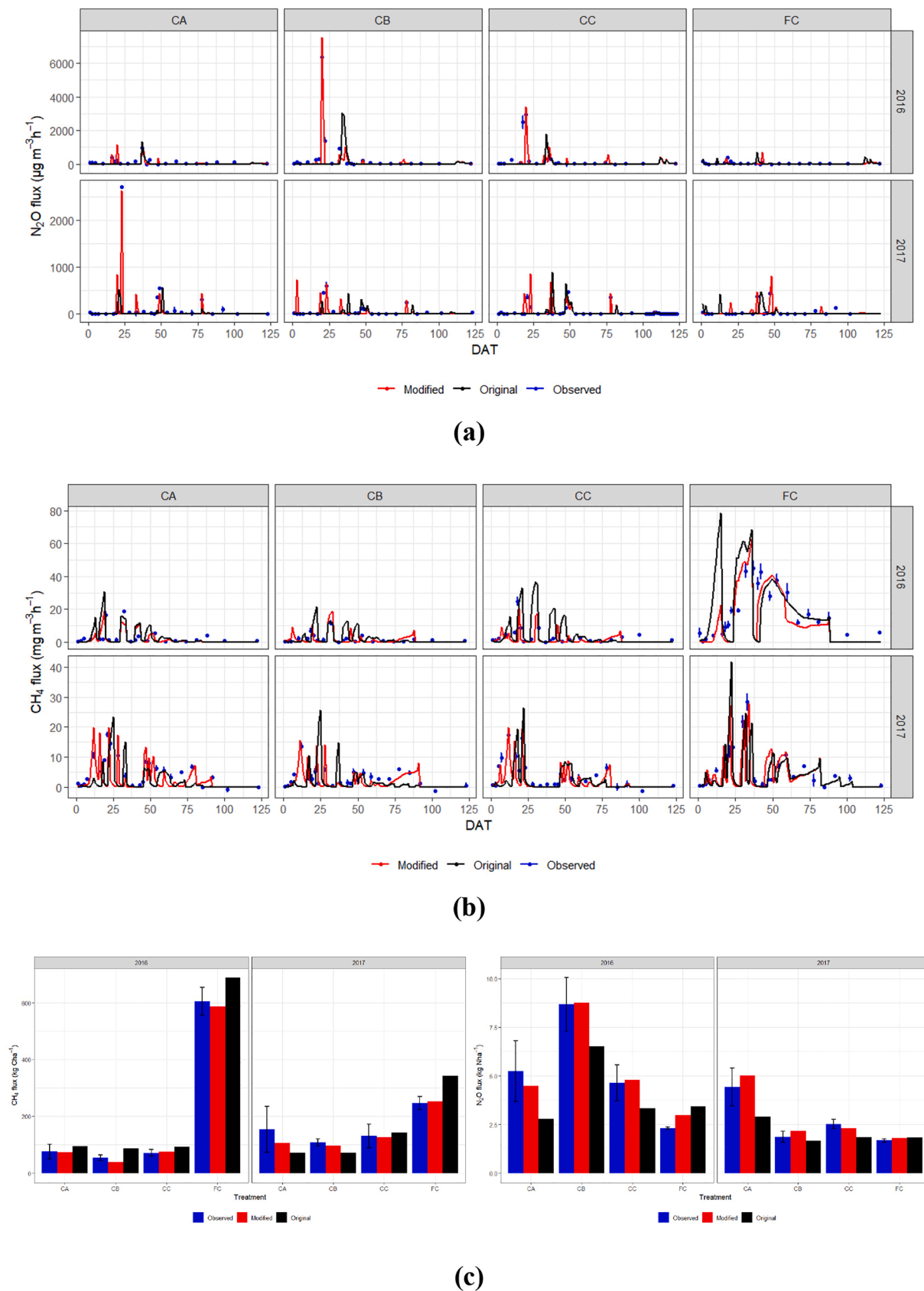


**Fig. 3.** Comparison of the observed, simulated CH<sub>4</sub> (a), N<sub>2</sub>O (b) and cumulative emissions (c) from paddy fields under different biochar applications and irrigation by original model and DNDC-BC in calibration period (2016) and validation period (2017).

**Table 5**  
Statistical criteria for simulation of CH<sub>4</sub> and N<sub>2</sub>O emissions.

GHG Models	Years	Treatments	N	R <sup>2</sup>		RMSE		nRMSE (%)		EF	
				DNDC-BC	DNDC	DNDC-BC	DNDC	DNDC-BC	DNDC	DNDC-BC	DNDC
CH <sub>4</sub>	2016	CA	22	0.83	0.67	2.18	3.05	16.12	21.73	0.84	0.63
		CB	22	0.81	0.66	2.20	2.71	16.45	28.67	0.82	0.67
		CC	22	0.79	0.61	2.59	4.32	22.65	27.72	0.81	0.56
		FC	22	0.87	0.69	1.41	4.25	9.39	27.33	0.87	0.60
	2017	CA	22	0.82	0.63	2.56	2.99	21.39	28.87	0.83	0.63
		CB	22	0.82	0.60	2.15	2.32	19.08	29.37	0.83	0.52
		CC	22	0.86	0.64	1.55	2.30	18.23	26.95	0.86	0.61
		FC	22	0.93	0.72	1.17	2.16	14.38	18.05	0.93	0.59
N <sub>2</sub> O	2016	CA	25	0.89	0.52	62.04	84.30	7.81	21.06	0.87	0.52
		CB	25	0.91	0.54	58.26	77.70	4.31	21.47	0.92	0.49
		CC	25	0.84	0.51	78.31	96.56	9.79	25.65	0.83	0.47
		FC	25	0.83	0.53	75.12	96.46	10.21	25.65	0.82	0.51
	2017	CA	25	0.97	0.63	48.76	79.78	7.26	15.33	0.96	0.61
		CB	25	0.92	0.61	59.64	87.99	7.96	12.87	0.95	0.63
		CC	25	0.93	0.65	59.02	86.83	15.76	14.56	0.93	0.65
		FC	25	0.88	0.58	69.20	88.95	16.79	22.59	0.87	0.57

**Note:** N denotes the sample size. The RMSE units of CH<sub>4</sub> and N<sub>2</sub>O are mg m<sup>-2</sup>h<sup>-1</sup> and µg m<sup>-2</sup>h<sup>-1</sup>, respectively. 2016 and 2017 represent calibration and validation years respectively. CA, CB, CC, and FC represent 0, 20, 40, 40 t ha<sup>-1</sup> biochar application with CI (C) and FI (F), respectively.

#### 4.2. Effects of biochar and CI on soil environment, SOC and rice yield

DNDC-BC performed better than the DNDC model in simulating soil temperature and moisture, especially under CI conditions. Similar weak performance of soil moisture simulations by DNDC were also reported by Abdalla et al. (2022, 2020) for double and multiple cropping systems in China. A recent study by Guo et al. (2023) investigated CH<sub>4</sub> emissions and grain yield for paddy rice also recommended further improvement of the DNDC. This might be because the original version of DNDC simplifies the flood treatment. Moreover, the DNDC95 model doesn't include biochar as an input option for carbon management. By introducing parameters such as biochar pH, adsorption rate and C pools of biochar, the problem of poor performance of DNDC95 in simulating soil temperature and pH under biochar treatment has been resolved (Shaikat et al., 2022).

Carbon sequestration is another important issue when promoting a new farmland management practice. In this study, the coupling of biochar and CI increased SOC and boosted rice yield by 4.25%-19.27% and 9.35%-15.85%, respectively. Similar results were previously reported (Asai et al., 2009; Laird et al., 2010), partly because the stabilize structure of biochar inhibited the surface oxidation of SOC, reduced the mineralization rate and increased SOC (Yang et al., 2020; Jiang et al., 2021b). Biochar increases plant height, tillering and rice filled grain number thereby, increasing rice yield (Chen et al., 2021). Moreover, previous studies found that biochar can mitigate GHG emissions by reducing the positive activation energy and increasing the negative activation energy (Qi et al., 2020). This study found that N<sub>2</sub>O emission is positively correlated with precipitation, which may be due to the influence of soil moisture content on N<sub>2</sub>O production and emission mechanism, which is consistent with the conclusion of Chen et al. (2019) and Rudaz et al. (1999).

#### 4.3. Implications and limitations

The original DNDC95 model can neither simulate CI system controlled by soil moisture nor biochar application. In this study, the water balance equation and two-pool biochar model (i.e., DNDC-BC) were introduced to realize this function and simulate GHG emissions, SOC and rice yield from paddy systems under frequent wetting and drying and biochar amendments. The significant improvement in the simulated results of CH<sub>4</sub> and N<sub>2</sub>O justify the use of the DNDC-BC model to estimate GHG emissions from CI and FI paddy fields under biochar application treatments. The DNDC-BC has achieved a satisfactory performance in simulating soil environment, CH<sub>4</sub> and N<sub>2</sub>O emissions, SOC,

and rice yield, and therefore, could be used to accurately estimate GHG mitigation potential and hot spot distribution of paddy fields at a regional scale. This study showed the great potential of combined biochar-CI management, its role in GHG abatement, carbon sequestration, yield boost, and water saving. Thus, this combined management system should be promoted in the future, as it is inexpensive and efficient. The development of DNDC-BC integrated with biochar modelling and water balance is encouraging because it expands the existing functions of the original model and achieves a better performance. There have been numerous studies on biochar increasing crop yield and SOC (Nayak et al., 2015; Agegnehu et al., 2016), but most of them are based on short-term experiments, and there is almost no simulation study under biochar amendment, especially combined with CI. DNDC-BC is a suitable tool to explore the long-term impacts of biochar-CI combination on soil, crop and environmental systems and impacts of climate change.

However, there are also some limitations with this study. Since the DNDC-BC model was validated and calibrated using only two years of measured data and a dataset (22 sets from literature), there may be uncertainty in the long-term simulations. Thus, test data covering a longer period should be used to calibrate the model in the future research. The limited measurement duration is the result of biochar being a relatively new management technology and thus most biochar studies span over only a few measurement years. Whether those various carbon cycle processes will influence the simulation accuracy should be tested by CO<sub>2</sub> flux experiment in the future work as well. Actually, this is the first step in a long process of DNDC development for biochar, and more studies with detailed data (from different sites, longer years and soil depths) will follow. In addition, it should be noted that the improvement of soil water part in DNDC-BC is still limited. Though the simulation under CI was realized, the default bucket model framework of DNDC95 is still retained. Thus, the main limitations, such as simulating capillary rise from the retreating groundwater table and drainage flow, remain to be solved. In the future, it could be solved by combining other hydrological models, such as Hydrus 2D, or adding Richards equation, or introduce parameters including unsaturated flow above field capacity, heterogeneous soil profile, root development and tile drainage (Smith et al., 2020). The ability of two-pool biochar model to simulate soil mineralization has been proved (Leng et al., 2019), but it is still necessary to continue CO<sub>2</sub> flux experiment in the future to further verify and improve DNDC-BC. Although DNDC-BC performed well in general, there are still some areas that can be improved under FI conditions, such as overestimation of CH<sub>4</sub> peak at the initial stage. We speculated that the current model simplification, such as the biochar modelling of double C pools, could be further improved, and the

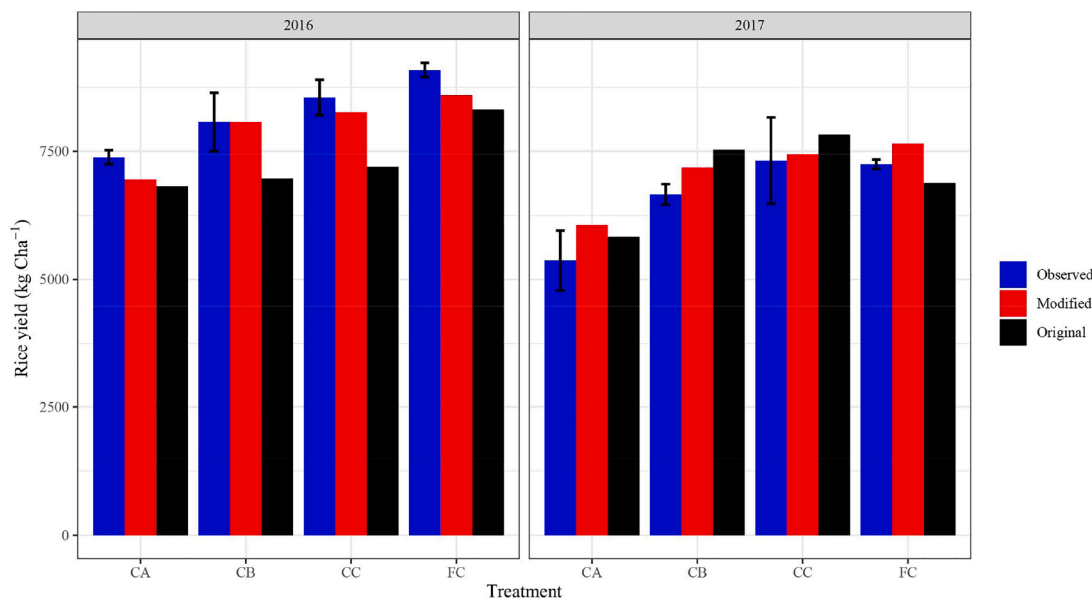
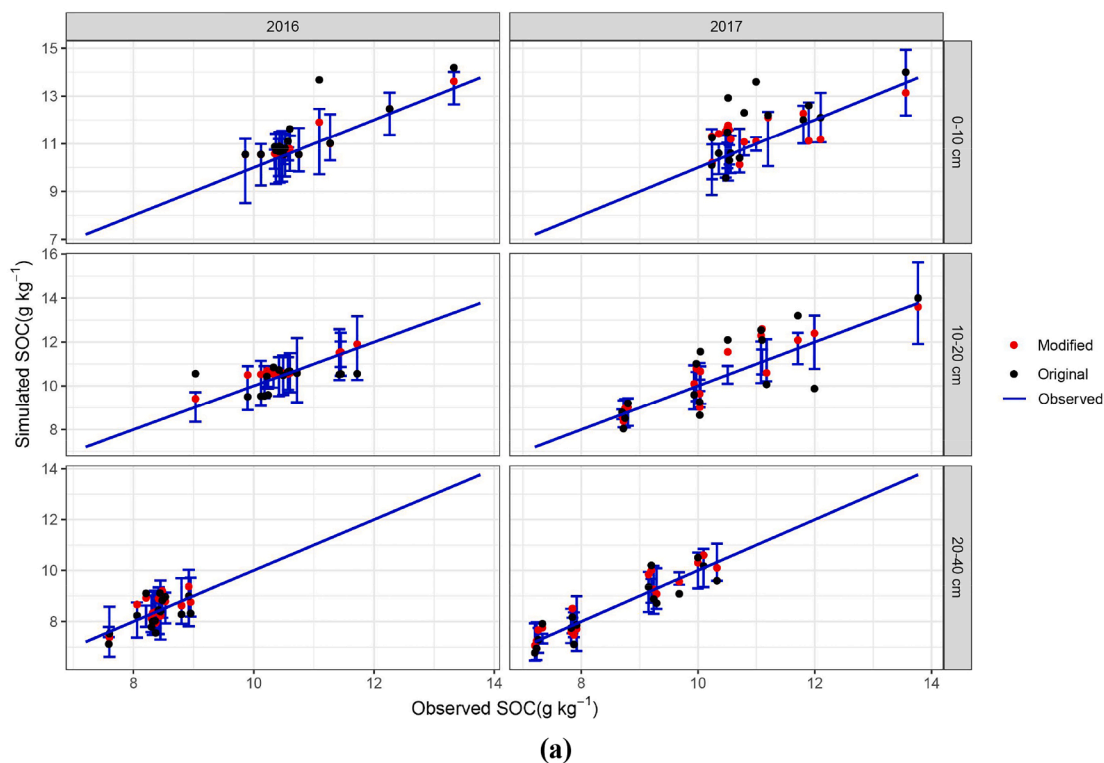


Fig. 4. Comparison of simulated and measured SOC and rice yield of each treatment in 2016 and 2017.

connection between C pool module and flooding module needs to be further improved. In the future, three-pool models of biochar could be developed and introduced into other biogeochemical models, considering that biochar has become a widely used soil improvement and negative emission management measure. In addition, it is interesting to use the DNDC-BC for predicting the impacts of climate change and exploring the long-term effects of CI and biochar application on GHG emissions, rice yield and SOC (Jiang et al., 2022; Martre et al., 2015).

5. Conclusions

Calibration and validation of our new approach, DNDC-BC, revealed that the model can simulate impacts of biochar-CI combination on CH<sub>4</sub>

and N<sub>2</sub>O emissions, SOC, and grain yield satisfactorily. The possible reasons for the mitigation of N<sub>2</sub>O emissions by biochar were the increase of NH<sub>4</sub><sup>+</sup>-N and the decrease of NO<sub>3</sub><sup>-</sup>-N. The DNDC-BC captured the dynamics of soil temperature, moisture and SOC in different soil depths, but underestimated soil temperature in 10 cm depth. Sensitivity analysis showed that the DNDC-BC was most sensitive to precipitation and irrigation when simulating CH<sub>4</sub> emissions; to N fertilization, precipitation and irrigation when simulating N<sub>2</sub>O emissions and to biochar application rates when simulating SOC. Although the model has been tested at multiple sites and demonstrated good performance, future studies should focus on further developing and applying DNDC-BC for predicting the long-term impacts of biochar-CI on crop productivity and soils for more locations and across a wider range of climate scenarios. This

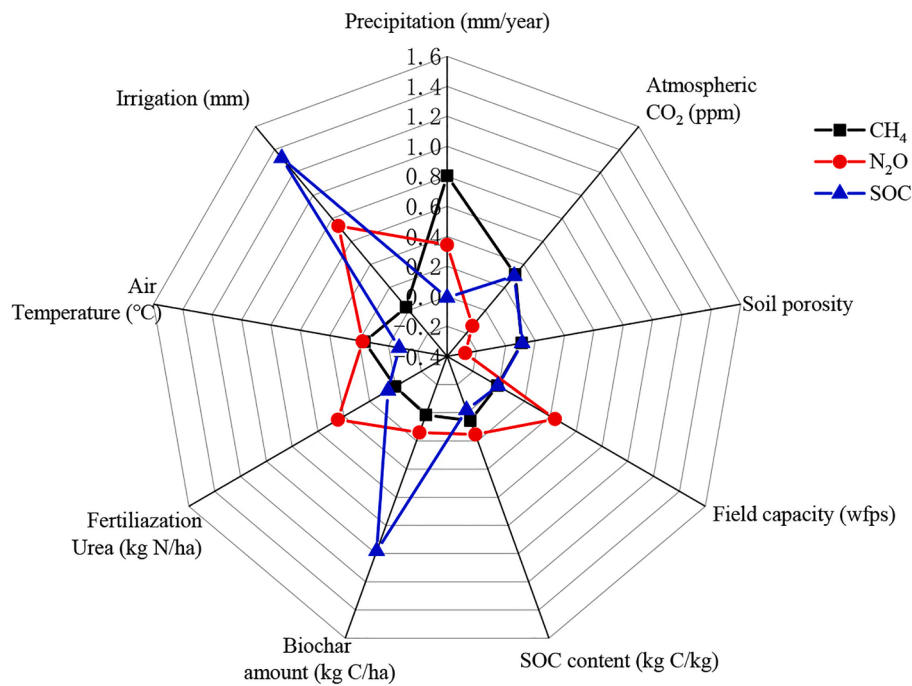


Fig. 5. Radar chart of sensitivity index of CH<sub>4</sub>, N<sub>2</sub>O emissions and SOC from paddy fields.

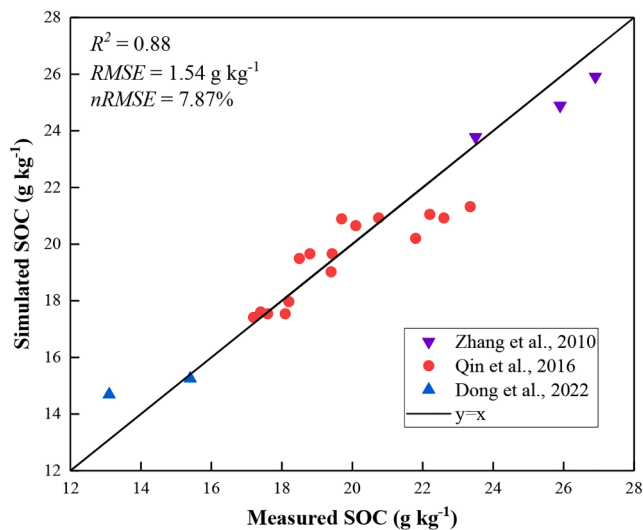


Fig. 6. Comparison of simulated and measured SOC at different sites by DNDC-BC. Detailed literature data can be obtained in Table S6.

will support decision-makers to advise on biochar-CI as a cost-effective management strategy for mitigating GHG emissions and reducing the contribution of croplands to climate change.

**CRediT authorship contribution statement**

**Zewei Jiang:** Conceptualization, Data curation, Software, Methodology, Validation, Writing – original draft. **Shihong Yang:** Methodology, Funding acquisition, Writing – review & editing. **Pete Smith:** Methodology, Writing – review & editing. **Mohamed Abdalla:** Software, Validation, Writing – review & editing. **Qingqing Pang:** Data curation, Writing – review & editing. **Yi Xu:** Visualization, Writing – review & editing. **Suting Qi:** Data curation, Investigation. **Jiazhen Hu:** Validation, Supervision.

**Declaration of Competing Interest**

The authors declare that they have no known competing financial interests or personal relationships that could have appeared to influence the work reported in this paper.

**Data availability**

Data will be made available on request.

**Acknowledgments**

This work was supported by the National Natural Science Foundation of China (51879076), SuperG (Nr: 774124; funded under EU Horizon 2020 programme), the Fundamental Research Funds for the Central Universities (B220203009), the Postgraduate Research & Practice Program of Jiangsu Province (KYCX22\_0669), the Water Conservancy Science and Technology Project of Jiangxi Province (202124ZDKT09). Thanks to the late Professor Changsheng Li who provided the source code of DNDC and corresponding support. We thank the China Scholarship Council (CSC) for providing a scholarship (202206710073) to Zewei Jiang.

**Appendix A. Supplementary data**

Supplementary data to this article can be found online at <https://doi.org/10.1016/j.geoderma.2023.116450>.

**References**

Abdalla, M., Kumar, S., Jones, M., Burke, J., Williams, M., 2011. Testing DNDC model for simulating soil respiration and assessing the effects of climate change on the CO<sub>2</sub> gas flux from Irish agriculture. *Global Planet. Change* 78 (3–4), 106–115.  
 Abdalla, M., Song, X., Ju, X., Topp, C.F.E., Smith, P., 2020. Calibration and validation of the DNDC model to estimate nitrous oxide emissions and crop productivity for a summer maize-winter wheat double cropping system in Hebei, China. *Environ. Pollut.* 262, 114199.  
 Abdalla, M., Song, X., Ju, X., Smith, P., 2022. Evaluation of the DNDC Model to Estimate Soil Parameters, Crop Yield and Nitrous Oxide Emissions for Alternative Long-Term Multi-Cropping Systems in the North China Plain. *Agronomy* 12 (1), 109.

- Agegnehu, G., Bass, A.M., Nelson, P.N., Bird, M.I., 2016. Benefits of biochar, compost and biochar-compost for soil quality, maize yield and greenhouse gas emissions in a tropical agricultural soil. *Sci. Total Environ.* 543, 295–306.
- Akhtar, S.S., Li, G., Andersen, M.N., Liu, F., 2014. Biochar enhances yield and quality of tomato under reduced irrigation. *Agric Water Manag* 138, 37–44.
- Allen, R.G., Pereira, L.S., Raes, D., Smith, M., 1998. Crop evapotranspiration-Guidelines for computing crop water requirements-FAO Irrigation and drainage paper 56. *Fao, Rome* 300 (9), D05109.
- Allen, R.G., Pruitt, W.O., Wright, J.L., Howell, T.A., Ventura, F., Snyder, R., Itenfisu, D., Steduto, P., Berengena, J., Yrisary, J.B., 2006. A recommendation on standardized surface resistance for hourly calculation of reference ET<sub>o</sub> by the FAO56 Penman-Monteith method. *Agric Water Manag* 81 (1–2), 1–22.
- Asai, H., Samson, B.K., Stephan, H.M., Songyikhangsuthor, K., Homma, K., Kiyono, Y., Inoue, Y., Shiraiwa, T., Horie, T., 2009. Biochar amendment techniques for upland rice production in Northern Laos. *Field Crop Res* 111 (1–2), 81–84.
- Bradford, M.A., Wieder, W.R., Bonan, G.B., Fierer, N., Raymond, P.A., Crowther, T.W., 2016. Managing uncertainty in soil carbon feedbacks to climate change. *Nat. Clim. Chang.* 6 (8), 751–758.
- Carlson, K.M., Gerber, J.S., Mueller, N.D., Herrero, M., MacDonald, G.K., Brauman, K.A., Havlik, P., O'Connell, C.S., Johnson, J.A., Saatchi, S., West, P.C., 2016. Greenhouse gas emissions intensity of global croplands. *Nat. Clim. Chang.* 7 (1), 63–68.
- Chen, T., Oenema, O., Li, J., Misselbrook, T., Dong, W., Qin, S., Yuan, H., Li, X., Hu, C., 2019. Seasonal variations in N<sub>2</sub> and N<sub>2</sub>O emissions from a wheat–maize cropping system. *Biol. Fertil. Soils* 55 (6), 539–551.
- Chen, L., Wang, Z., Wei, C., Gao, M., 2009. Discussion on Dynamics Models of Soil Organic Carbon and Soil Organic Nitrogen. *Chin. J. Soil Sci.* 40 (2), 432–438.
- Chen, X., Yang, S., Ding, J., Jiang, Z., Sun, X., 2021. Effects of Biochar Addition on Rice Growth and Yield under Water-Saving Irrigation. *Water* 13 (2), 209.
- De Feudis, M., Cardelli, V., Massaccesi, L., Trumbore, S.E., Vittori Antisari, L., Cocco, S., Corti, G., Agnelli, A., 2019. Small altitudinal change and rhizosphere affect the SOM light fractions but not the heavy fraction in European beech forest soil. *Catena* 181, 104091.
- Dubache, G., Li, S., Zheng, X., Zhang, W., Deng, J., 2019. Modeling ammonia volatilization following urea application to winter cereal fields in the United Kingdom by a revised biogeochemical model. *Sci. Total Environ.* 660, 1403–1418.
- Fidel, R.B., Laird, D.A., Parkin, T.B., 2017. Impact of six lignocellulosic biochars on C and N dynamics of two contrasting soils. *GCB Bioenergy* 9 (7), 1279–1291.
- Gilhespy, S.L., Anthony, S., Cardenas, L., Chadwick, D., del Prado, A., Li, C., Misselbrook, T., Rees, R.M., Salas, W., Sanz-Cobena, A., Smith, P., Tilston, E.L., Topp, C.F.E., Vetter, S., Yeluripati, J.B., 2014. First 20 years of DNDC (DeNitrification DeComposition): Model evolution. *Ecol. Model.* 292, 51–62.
- Guo, F., Zhang, J., Yang, X., He, Q., Ao, L., Chen, Y., 2020. Impact of biochar on greenhouse gas emissions from constructed wetlands under various influent chemical oxygen demand to nitrogen ratios. *Bioresour. Technol.* 303, 122908.
- Guo, Y., Zhang, G., Abdalla, M., Kuhnert, M., Bao, H., Xu, H., Ma, J., Begum, K., Smith, P., 2023. Modelling methane emissions and grain yields for a double-rice system in Southern China with DAYCENT and DNDC models. *Geoderma* 431, 116364.
- Haque, A.N.A., Uddin, M.K., Sulaiman, M.F., Amin, A.M., Hossain, M., Solaiman, Z.M., Mosharraf, M., 2021. Biochar with Alternate Wetting and Drying Irrigation: A Potential Technique for Paddy Soil Management. *Agriculture* 11 (4), 367.
- He, X., Han, L., Fu, B., Du, S., Liu, Y., Huang, G., 2019. Effect and microbial reaction mechanism of rice straw biochar on pore methane production during mainstream large-scale aerobic composting in China. *J. Clean. Prod.* 215, 1223–1232.
- He, Y., Liang, H., Hu, K., Wang, H., Hou, L., 2018. Modeling nitrogen leaching in a spring maize system under changing climate and genotype scenarios in arid Inner Mongolia, China. *Agric Water Manag* 210, 316–323.
- Hou, H., Peng, S., Xu, J., Yang, S., Mao, Z., 2012. Seasonal variations of CH<sub>4</sub> and N<sub>2</sub>O emissions in response to water management of paddy fields located in Southeast China. *Chemosphere* 89 (7), 884–892.
- Islam, S.F., van Groenigen, J.W., Jensen, L.S., Sander, B.O., de Neergaard, A., 2018. The effective mitigation of greenhouse gas emissions from rice paddies without compromising yield by early-season drainage. *Sci. Total Environ.* 612, 1329–1339.
- Jiang, Z., Yang, S., Ding, J., Sun, X., Chen, X., Liu, X., Xu, J., 2021a. Modeling Climate Change Effects on Rice Yield and Soil Carbon under Variable Water and Nutrient Management. *Sustainability* 13 (2), 568.
- Jiang, Z., Yang, S., Pang, Q., Xu, Y., Chen, X., Sun, X., Qi, S., Yu, W., 2021b. Biochar improved soil health and mitigated greenhouse gas emission from controlled irrigation paddy field: Insights into microbial diversity. *J. Clean. Prod.* 318, 128595.
- Jiang, Z., Yang, S., Liu, Z., Xu, Y., Shen, T., Qi, S., Pang, Q., Xu, J., Liu, F., Xu, T., 2022. Can ensemble machine learning be used to predict the groundwater level dynamics of farmland under future climate: a 10-year study on Huaibei Plain. *Environ. Sci. Pollut. Res. Int.* 29, 44653–44667.
- Kuzyakov, Y., Bogomolova, I., Glaser, B., 2014. Biochar stability in soil: Decomposition during eight years and transformation as assessed by compound-specific <sup>14</sup>C analysis. *Soil Biol. Biochem.* 70, 229–236.
- Laird, D.A., Fleming, P., Davis, D.D., Horton, R., Wang, B., Karlen, D.L., 2010. Impact of biochar amendments on the quality of a typical Midwestern agricultural soil. *Geoderma* 158 (3–4), 443–449.
- Lehmann, J., 2007. A handful of carbon. *Nature* 447 (7141), 143–144.
- Lehmann, J., Joseph, S., 2009. Biochar for environmental management: An introduction. *Biochar for environmental management. Science and technology.* Earthscan Publishers Ltd.
- Leng, L., Huang, H., 2018. An overview of the effect of pyrolysis process parameters on biochar stability. *Bioresour. Technol.* 270, 627–642.
- Leng, L., Xu, X., Wei, L., Fan, L., Huang, H., Li, J., Lu, Q., Li, J., Zhou, W., 2019. Biochar stability assessment by incubation and modelling: Methods, drawbacks and recommendations. *Sci. Total Environ.* 664, 11–23.
- Li, C., Froliking, S., Froliking, T.A., 1992a. A model of nitrous oxide evolution from soil driven by rainfall events: 1. Model structure and sensitivity. *J. Geophys. Res. Atmos.* 97 (D9), 9759–9776.
- Li, C., Froliking, S., Froliking, T.A., 1992b. A model of nitrous oxide evolution from soil driven by rainfall events: 2. Model applications. *J. Geophys. Res.: Atmos.* 97 (D9), 9777–9783.
- Li, H., Wang, L., Qiu, J., Li, C., Gao, M., Gao, C., 2014. Calibration of DNDC model for nitrate leaching from an intensively cultivated region of Northern China. *Geoderma* 223–225, 108–118.
- Li, H., Meng, J., Liu, Z., Lan, Y., Yang, X., Huang, Y., He, T., Chen, W., 2021. Effects of biochar on N<sub>2</sub>O emission in denitrification pathway from paddy soil: A drying incubation study. *Sci. Total Environ.* 787, 147591.
- Liang, H., Hu, K., Qin, W., Zuo, Q., Zhang, Y., 2017. Modelling the effect of mulching on soil heat transfer, water movement and crop growth for ground cover rice production system. *Field Crop Res* 201, 97–107.
- Liang, K., Zhong, X., Huang, N., Lampayan, R.M., Pan, J., Tian, K., Liu, Y., 2016. Grain yield, water productivity and CH<sub>4</sub> emission of irrigated rice in response to water management in south China. *Agric Water Manag* 163, 319–331.
- Martre, P., Wallach, D., Asseng, S., Ewert, F., Jones, J.W., Rotter, R.P., Boote, K.J., Ruane, A.C., Thorburn, P.J., Cammarano, D., Hatfield, J.L., Rosenzweig, C., Aggarwal, P.K., Angulo, C., Basso, B., Bertuzzi, P., Biernath, C., Brisson, N., Challinor, A.J., Doltra, J., Gayler, S., Goldberg, R., Grant, R.F., Heng, L., Hooker, J., Hunt, L.A., Ingwersen, J., Izaurralde, R.C., Kersebaum, K.C., Muller, C., Kumar, S.N., Nendel, C., O'Leary, G., Olesen, J.E., Osborne, T.M., Palosuo, T., Priesack, E., Ripoche, D., Semenov, M.A., Shcherbak, I., Steduto, P., Stockle, C.O., Stratonovitch, P., Streck, T., Supit, I., Tao, F., Travasso, M., Waha, K., White, J.W., Wolf, J., 2015. Multimodel ensembles of wheat growth: many models are better than one. *Glob. Chang. Biol.* 21 (2), 911–925.
- Nan, Q., Xin, L., Qin, Y., Waqas, M., Wu, W., 2021. Exploring long-term effects of biochar on mitigating methane emissions from paddy soil: a review. *Biochar* 3 (2), 125–134.
- Nayak, D., Saetnan, E., Cheng, K., Wang, W., Koslowski, F., Cheng, Y.-F., Zhu, W.Y., Wang, J.-K., Liu, J.-X., Moran, D., Yan, X., Cardenas, L., Newbold, J., Pan, G., Lu, Y., Smith, P., 2015. Management opportunities to mitigate greenhouse gas emissions from Chinese agriculture. *Agr. Ecosyst Environ* 209, 108–124.
- Peng, S., Zhang, Z., Pang, G., 2009. Mechanical evaluation and cause analysis of rice-stem lodging resistance under controlled irrigation in cold region. *Trans. Chin. Soc. Agric. Eng.* 25 (1), 6–10.
- Qi, L., Pokharel, P., Ni, C., Gong, X., Zhou, P., Niu, H., Wang, Z., Gao, M., 2020. Biochar changes thermal activation of greenhouse gas emissions in a rice–lettuce rotation microcosm experiment. *J. Clean. Prod.* 247.
- Rudaz, A., Wälti, E., Kyburz, G., Lehmann, P., Fuhrer, J., 1999. Temporal variation in N<sub>2</sub>O and N<sub>2</sub> fluxes from a permanent pasture in Switzerland in relation to management, soil water content and soil temperature. *Agr. Ecosyst Environ* 73, 83–91.
- Shaukat, M., Muhammad, S., Maas, E.D.V.L., Khaliq, T., Ahmad, A., 2022. Predicting methane emissions from paddy rice soils under biochar and nitrogen addition using DNDC model. *Ecol. Model.* 466, 109896.
- Si, T., Wang, H., Zhang, W., 2000. Discussion and suggestions on rice water saving in China. *J. Irrig. Drain.* 19 (1), 30–33.
- Singh, N., Abiven, S., Torn, M.S., Schmidt, M.W.I., 2012. Fire-derived organic carbon in soil turns over on a centennial scale. *Biogeochemistry* 9 (8), 2847–2857.
- Smith, W., Grant, B., Qi, Z., He, W., VanderZaag, A., Drury, C.F., Helmers, M., 2020. Development of the DNDC model to improve soil hydrology and incorporate mechanistic tile drainage: A comparative analysis with RZWQM2. *Environ. Model. Softw.* 123, 104577.
- Song, T., Xu, F., Yuan, W., Chen, M., Hu, Q., Tian, Y., Zhang, J., Xu, W., 2019. Combining alternate wetting and drying irrigation with reduced phosphorus fertilizer application reduces water use and promotes phosphorus use efficiency without yield loss in rice plants. *Agric Water Manag* 223, 105686.
- US-EPA, 2006. Global anthropogenic non-CO<sub>2</sub> greenhouse gas emissions: 1990–2020, United States Environmental Protection Agency, Washington, DC. (ONLINE Available at):<http://www.epa.gov/nonco2/econinv/downloads/GlobalAnthroEmissionsReport.pdf> (EPA 430-R-06-003, June 2006)(Accessed 18.09.16).
- Yang, S., Xiao, Y., Sun, X., Ding, J., Jiang, Z., Xu, J., 2019. Biochar improved rice yield and mitigated CH<sub>4</sub> and N<sub>2</sub>O emissions from paddy field under controlled irrigation in the Taihu Lake Region of China. *Atmos. Environ.* 200, 69–77.
- Yang, S., Chen, X., Jiang, Z., Ding, J., Sun, X., Xu, J., 2020. Effects of Biochar Application on Soil Organic Carbon Composition and Enzyme Activity in Paddy Soil under Water-Saving Irrigation. *Int. J. Environ. Res. Public Health* 17 (1), 333.
- Yang, J., Yang, J., Liu, S., Hoogenboom, G., 2014. An evaluation of the statistical methods for testing the performance of crop models with observed data. *Agr. Syst.* 127, 81–89.
- Yin, J., Zhao, L., Xu, X., Li, D., Qiu, H., Cao, X., 2022. Evaluation of long-term carbon sequestration of biochar in soil with biogeochemical field model. *Sci. Total Environ.* 822, 153576.
- Zhang, Y., Niu, H., 2016. The development of the DNDC plant growth sub-model and the application of DNDC in agriculture: A review. *Agr. Ecosyst. Environ* 230, 271–282.
- Zhao, Z., Wu, S., Zhou, D., Chu, C., Cao, L., 2016. Modeling N loss from paddy fields and sensitivity analysis with DNDC model. *J. Agro-Environ. Sci.* 35 (12), 2405–2412.